

Document downloaded from:

<http://hdl.handle.net/10251/28319>

This paper must be cited as:

Banyasz, A.; Vayá Pérez, I.; Changenet-Barret, P.; Gustavsson, T.; Douki, T.; Markovitsi, D. (2011). Base Pairing Enhances Fluorescence and Favors Cyclobutane Dimer Formation Induced upon Absorption of UVA Radiation by DNA. *Journal of the American Chemical Society*. 133:5163-5165. doi:10.1021/ja110879m



The final publication is available at

<http://dx.doi.org/10.1021/ja110879m>

Copyright American Chemical Society

Additional Information

# Base-pairing enhances fluorescence and favors cyclobutane dimer formation induced upon absorption of UVA radiation by DNA

Akos Banyasz, Ignacio Vayá, Pascale Changenet-Barret, Thomas Gustavsson, Thierry Douki and Dimitra Markovitsi\*

Laboratoire Francis Perrin, CEA/IRAMIS/SPAM - CNRS URA 2453, 91191 Gif-sur-Yvette, France and CEA, INAC, SCIB, UJF & CNRS, LCIB (UMR\_E 3 CEA-UJF and FRE 3200), Laboratoire « Lésions des Acides Nucléiques », 17 Rue des Martyrs, F-38054 Grenoble Cedex 9, France.

RECEIVED DATE (automatically inserted by publisher); dimitra.markovitsi@cea.fr

**Abstract.** The photochemical properties of the DNA duplex  $(dA)_{20} \cdot (dT)_{20}$  are compared with those of the parent single strands. It is shown that base-pairing increases the probability of absorbing UVA photons, probably due to the formation of charge transfer states. UVA excitation induces fluorescence peaking at ca. 420 nm and decaying on the nanosecond time-scale. The fluorescence quantum yield, the fluorescence lifetime and the quantum yield for cyclobutane dimer formation increase upon base-pairing. Such behavior contrasts with that of the UVC-induced processes.

The knowledge that absorption of UV radiation by DNA induces carcinogenic mutations has triggered numerous studies aiming at the characterization of its electronic excited states and their relaxation dynamics.<sup>1,2</sup> All these investigations consider UVC or UVB excitation but their UVA counterpart has not yet been addressed. This is due to the fact that individual DNA bases do not absorb UVA radiation. However, a few studies have shown that this is not true for duplexes which indeed present a weak absorption tail above 300 nm.<sup>3,4</sup> Moreover, it has been pointed out that absorption of UVA radiation by natural isolated and genomic DNA and by the synthetic duplex  $(dA)_{20} \cdot (dT)_{20}$  leads to the formation of the highly mutagenic cyclobutane pyrimidine dimers (CPDs).<sup>4,5</sup> This is an important issue because UVA photons are much more abundant than those of UVC or UVB in the solar radiation reaching the surface of the Earth.<sup>6</sup> Here we report the first fluorescence study with UVA excitation performed for  $(dA)_{20} \cdot (dT)_{20}$  and the parent single strands  $(dA)_{20}$  and  $(dT)_{20}$ . We also determine the quantum yields for CPD formation for which no information was available so far regarding the UVA range. We show that base-pairing enhances fluorescence and favors CPD formation which contrasts with the effect of UVC irradiation.

The DNA strands dissolved in phosphate buffer (0.1 M  $\text{NaH}_2\text{PO}_4$ , 0.1 M  $\text{Na}_2\text{HPO}_4$  and 0.25 M NaCl) were studied at room temperature. Strand concentrations ranging from  $3 \times 10^{-6}$  M to  $10^{-4}$  M were used. In order to rule out that the UVA-induced fluorescence and CPDs are not related to impurities we performed a series of control experiments described in detail in the supporting information. Briefly, we tested nucleic acids from different suppliers, different purification methods and different types of added salts. Fluorescence decays were obtained by time-correlated single photon counting (TCSPC). The excitation source was the second (365 nm) or the third (267 nm) harmonic of a tunable Ti-sapphire laser (120 fs fwhm at 800 nm). Irradiations were carried out using the Xenon arc lamp of a

Fluorolog-3 spectrofluorimeter (SPEX, Jobin-Yvon). Formation of thymine dimers was monitored by high performance liquid chromatography coupled to mass spectrometry.

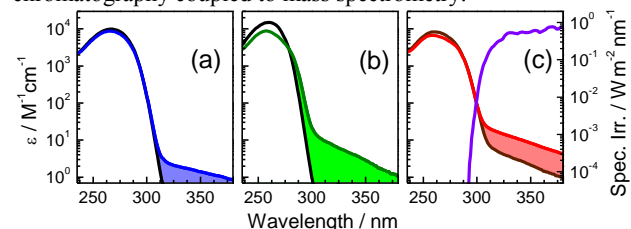


**Figure 1.** Comparison of the absorption spectra of  $(dT)_{20}$  (blue) and  $(dA)_{20}$  (green) with the corresponding monomeric chromophores (black) dT and dA (a and b) on the one hand, and the spectrum of the duplex  $(dA)_{20} \cdot (dT)_{20}$  (red) with that corresponding to the sum of the  $(dT)_{20}$  and  $(dA)_{20}$  spectrum (brown, c), on the other. The molar absorption coefficient  $\epsilon$  is given per base. In violet: a typical solar spectrum.<sup>6</sup>

The absorption spectra of the single strands  $(dT)_{20}$  and  $(dA)_{20}$ , (Figures 1a and 1b), exhibit a weak long wavelength tail which extends all over the whole UVA region and is absent from the spectra of the corresponding monomeric chromophores, thymidine (dT) and 2'-deoxyadenosine (dA), respectively. The molar absorption coefficient per base determined for the duplex in the UVA spectral domain is higher than that corresponding to the sum of the parent single strands (Figure 1c). These findings clearly show that the UVA absorption arises from interchromophore interactions which are expected to increase in the order:  $(dT)_{20}$ ,  $(dA)_{20}$  and  $(dA)_{20} \cdot (dT)_{20}$  as a result of a better chromophore organization and reduced conformational motions. Electronic coupling between dipolar  $\pi\pi^*$  transitions of the DNA bases is known to give rise to exciton states whose properties differ from those of single chromophores.<sup>7</sup> The strength of the dipolar coupling for stacked or paired bases does not exceed a few hundreds of wavenumbers.<sup>8</sup> Consequently, it is very unlikely that Frenkel excitons are encountered at such low energies. Furthermore,  $\pi\pi^*$  states, which have the lowest energy for DNA bases in the gas phase, are expected to be strongly destabilized in the presence of water molecules.<sup>1</sup> In contrast, the occurrence of charge transfer (CT) states in the UVA region is quite plausible. Several theoretical studies dealing with small double-stranded structures have reported the existence of CT states, involving bases located either in the same or in different strands, but positioned the related transitions at shorter wavelengths.<sup>9,10</sup> However, CT states can be strongly stabilized in aqueous solution. They are very sensitive to conformational and environmental factors which may modulate their energy and

thus spread the corresponding transitions over a larger spectral range.<sup>10</sup>

The emission maxima of all the examined oligonucleotides obtained upon UVA excitation range between 415 and 430 nm (Figure 2 and Table 1). Interestingly, similar bands have been observed upon UVC excitation of the alternating duplex (dAdT)<sub>10</sub>·(dAdT)<sub>10</sub> and the adenine dinucleotide; they were attributed to exciplex/excimer emission.<sup>11</sup> They are not altered when the solutions are saturated by nitrogen or oxygen, precluding any emission from triplet states.

The overlap between the UVA- and UVC-induced fluorescence spectra suggests that the excited states emitting at *ca.* 420 nm could be populated indirectly during the relaxation of  $\pi\pi^*$  excited states. However, in the latter case, other deactivation routes are dominant, as shown by the fluorescence quantum yields. Those determined upon UVA excitation for the single strands are about ten times higher than their UVC counterpart whereas, in the case of the duplex, the difference amounts nearly to two orders of magnitude (Table 1). In the case of UVA excitation, base pairing enhances fluorescence emission which does not happen for UVC excitation.

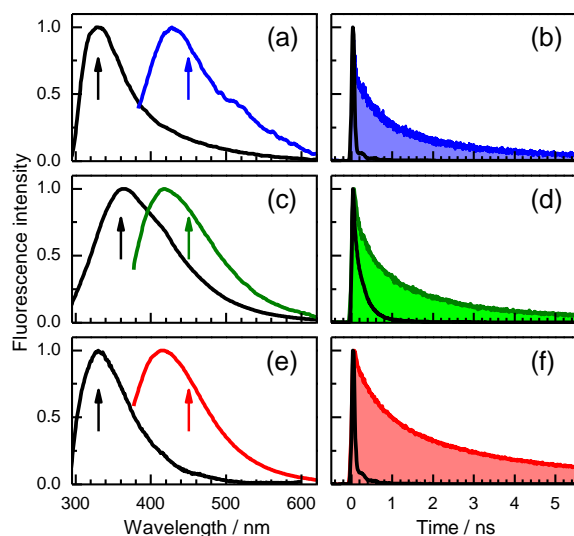


**Figure 2.** UVA-induced fluorescence properties of (dT)<sub>20</sub> (a, b; blue), (dA)<sub>20</sub> (c, d; green) and (dA)<sub>20</sub>·(dT)<sub>20</sub> (e, f; red). Normalized fluorescence spectra (a, c, e; excitation wavelength: 330 nm) and fluorescence decays (b, d, f; excitation wavelength: 365 nm). The corresponding properties induced by UVC excitation (267 nm) are shown in black. Arrows denote the emission wavelength at which the decays were recorded.

The UVA-induced fluorescence decays on the nanosecond time scale and is strongly non-exponential. Fits with four-exponential functions (supporting information) allowed us to determine the average fluorescence lifetimes  $\langle\tau_f\rangle$  and estimate the average radiative lifetimes  $\langle\tau_{rad}\rangle$  (Table 1). The  $\langle\tau_{rad}\rangle$  values range from 66 to 320 ns, corresponding to weakly allowed electronic transitions, in line with what is expected for CT excited states. Yet, the  $\langle\tau_{rad}\rangle$  values decrease successively when going from (dT)<sub>20</sub> to (dA)<sub>20</sub>, and further to (dA)<sub>20</sub>·(dT)<sub>20</sub>. This indicates that the greater the structural order the more allowed the electronic transitions related to the emission. We recall that we observed the same trend for the Franck-Condon transitions (Figure 1), which indicates a correlation between the excited states corresponding to photon absorption and photon emission.

The  $\langle\tau_{rad}\rangle$  values determined for (dT)<sub>20</sub> and (dA)<sub>20</sub>·(dT)<sub>20</sub> upon UVC excitation amounts to only a few ns, as expected for emission dominated by allowed  $\pi\pi^*$  transitions. A much higher  $\langle\tau_{rad}\rangle$  value is found for the UVC induced fluorescence of (dA)<sub>20</sub> which has been attributed to excimers.<sup>12</sup>

Focusing on (dT)<sub>20</sub> and (dA)<sub>20</sub>·(dT)<sub>20</sub>, in which thymine dimers can be formed, we compare the reaction products induced by UVA and UVC irradiation. As was previously reported for UVA irradiation of (dA)<sub>20</sub>·(dT)<sub>20</sub>, isolated genomic and cellular DNA,<sup>4</sup> only CPDs are detected also in the case of (dT)<sub>20</sub>. Neither (6-4) adducts nor Dewar valence isomers are found. The quantum yields of the UVA-induced CPDs are much lower than those determined following UVC irradiation<sup>13</sup> (Table 1). Despite their low values they are easily detectable by the analytical tools used to this end (supporting information). Taking into account the sensitivity of our measurements, we estimate that the quantum yield for the formation of (6-4) adducts is lower than 10<sup>-7</sup>.

A striking difference between UVC- and UVA-induced CPD formation is that, in the former case, base-pairing results in a twofold decrease of the quantum yield<sup>13</sup> whereas in the latter, the quantum yield increases nearly by one order of magnitude. The UVA case is surprising since, in principle, part of the absorbed UVA photons populate excited states located on adenines. Such an effect, together with the absence of other dimeric photoproducts, proves that UVA induction of CPDs occurs via a different mechanism than in the case of UVC. Theoretical calculations have shown that CPD formation induced by UVC radiation in (dT)<sub>20</sub> and (dA)<sub>20</sub>·(dT)<sub>20</sub>, which populates  $\pi\pi^*$  states, is governed by the ground state geometry.<sup>13</sup> In the case of UVA, the excited state relaxation obviously plays a crucial role. However, even in this case, the ground state geometry could be involved in an indirect way because it determines the conformations that give rise to UVA absorption.

We hope that the results presented here will inspire further experimental and theoretical work which will provide a detailed mechanism describing the UVA-induced reactivity of DNA. In particular, it would be interesting to explore the possible interconversion between CT and  $\pi\pi^*$  states, already reported for stacked adenines,<sup>14</sup> in the case of double stranded structures.

**Table 1.** Effect of UVA and UVC radiation on the properties of the emitting excited states and the reaction products determined for (dT)<sub>20</sub> and (dA)<sub>20</sub> and (dA)<sub>20</sub>·(dT)<sub>20</sub>, noted as T, A and A:T, respectively.

	UVA			UVC		
	T	A	A:T	T	A	A:T
$\lambda_{fl,max}$ (nm)	430 <sup>a)</sup>	420 <sup>a)</sup>	415 <sup>a)</sup>	330 <sup>b)</sup>	362 <sup>b)</sup>	330 <sup>b)</sup>
$\phi_f$ (10 <sup>-3</sup> )	2 <sup>a)</sup>	5 <sup>a)</sup>	20 <sup>a)</sup>	0.2 <sup>b)</sup>	0.6 <sup>b)</sup>	0.3 <sup>b)</sup>
$\langle\tau_f\rangle$ (ps)	640 <sup>c)</sup>	670 <sup>c)</sup>	1300 <sup>c)</sup>	0.7 <sup>d,e)</sup>	86 <sup>d)</sup>	2.4 <sup>d)</sup>
$\langle\tau_{rad}\rangle$ (ns)	320	130	66	3.5	143	8
$\phi_{CPD}$ (10 <sup>-3</sup> )	0.07 <sup>f)</sup>	-	0.5 <sup>f)</sup>	50 <sup>d)</sup>	-	22 <sup>d)</sup>
$\phi_{(6-4)}$ (10 <sup>-3</sup> )	<10 <sup>-4</sup> <sup>f)</sup>	-	<10 <sup>-4</sup> <sup>f)</sup>	5 <sup>d)</sup>	-	1.3 <sup>d)</sup>

$\lambda_{fl,max}$ : maximum of the fluorescence spectrum;  $\phi_f$ : fluorescence quantum yield;  $\langle\tau_f\rangle$ : average fluorescence lifetime;  $\langle\tau_{rad}\rangle$ : average radiative lifetime;  $\phi_{CPD}$ : quantum yield for CPD formation;  $\phi_{(6-4)}$ : quantum yield for the formation of (6-4) adducts; <sup>a)</sup>  $\lambda_{exc}$ : 330 nm; <sup>b)</sup>  $\lambda_{exc}$ : 255 nm; <sup>c)</sup>  $\lambda_{exc}$ : 365 nm; <sup>d)</sup>  $\lambda_{exc}$ : 267 nm; <sup>e)</sup> from ref.<sup>15</sup>; <sup>f)</sup>  $\lambda_{exc}$ : 335 and 354 nm.

**Acknowledgment** We thank Mrs Sz. Karpati and M. Perron for their help, Dr R. Improta for helpful discussions and the French

Agency for Research (ANR PCV07\_ 194999) for financial support. I. Vayá acknowledges the Conselleria de Educacion- Generalitat Valenciana (VALi+D program, N° 20100331).

**Supporting Information Available** Materials; experimental set-up and procedures, fits of fluorescence decays.

#### References

- (1) Middleton, C. T.; de La Harpe, K.; Su, C.; Law, U. K.; Crespo-Hernández, C. E.; Kohler, B. *Ann. Rev. Phys. Chem.* 2009, *60*, 217-239.
- (2) Markovitsi, D.; Gustavsson, T.; Vayá, I. *J. Phys. Chem. Lett.* 2010, *1*, 3271-3276.
- (3) Sutherland, J. C.; Griffin, K. P. *Radiat. Res.* 1981, *86*, 399-410.
- (4) Mouret, S.; Philippe, C.; Gracia-Chantegrel, J.; Banyasz, A.; Karpati, S.; Markovitsi, D.; Douki, T. *Org. Biomol. Chem.* 2010, *8*, 1706-1711.
- (5) Douki, T.; Reynaud-Angelin, A.; Cadet, J.; Sage, E. *Biochemistry* 2003, *42*, 9221-9226; Kielbassa, C.; Roza, L.; Epe, B. *Carcinogenesis* 1997, *18*, 811-816; Mouret, S.; Baudouin, C.; Charveron, M.; Favier, A.; Cadet, J.; Douki, T. *Proc. Natl. Acad. Sci. USA* 2006, *103*, 13765-13770.
- (6) Diffey, B. L. *Methods* 2002, *28*, 4-13.
- (7) Bouvier, B.; Gustavsson, T.; Markovitsi, D.; Millié, P. *Chem. Phys.* 2002, *275*, 75-92; Bittner, E. R. *J. Chem. Phys.* 2006, *125*, 094909 (1-12); Burin, A. L.; Armbruster, M. E.; Hariharan, M.; Lewis, F. D. *Proc. Natl. Acad. Sci. USA* 2009, *106*, 989-994.
- (8) Nachtigallova, D.; Hobza, P.; Ritze, H. H. *Phys. Chem. Chem. Phys.* 2008, *10*, 5689-5697; Kozak, C. R.; Kistler, K. A.; Lu, Z.; Matsika, S. *J. Phys. Chem. B* 2010, *114*, 1674-1683.
- (9) Starikov, E. B. *Modern Phys. Lett. B* 2004, *18*, 825-831; Blancafort, L.; Migani, A. *J. Am. Chem. Soc.* 2007, *129*, 14540-+; Santoro, F.; Barone, V.; Improta, R. *J. Am. Chem. Soc.* 2009, *131*, 15232-15245.
- (10) Lange, A. W.; Herbert, J. M. *J. Am. Chem. Soc.* 2009, *131*, 3913-3922.
- (11) Kwok, W. M.; Ma, C. S.; Phillips, D. L. *J. Phys. Chem. B* 2009, *113*, 11527-11534; Stuhldreier, M. C.; Schüller, C.; Kleber, J.; Temps, F. In *Ultrafast Phenomena XVII*; Chergui, M., Jonas, D., Riedle, E., Schoenlein, R. W., Taylor, A., Eds.; Oxford University Press.
- (12) Kwok, W.-M.; Ma, C.; Phillips, D. L. *J. Am. Chem. Soc.* 2006, *128*, 11894-11905.
- (13) McCullagh, M.; Lewis, F.; Markovitsi, D.; Douki, T.; Schatz, G. C. *J. Phys. Chem. B* 2010, *114*, 5215-5221.
- (14) Improta, R.; Santoro, F.; Barone, V.; Lami, A. *J. Phys. Chem. A* 2009, *113*, 15346-15354.
- (15) Markovitsi, D.; Sharonov, A.; Onidas, D.; Gustavsson, T. *ChemPhysChem* 2003, *3*, 303-305.

# Table of Contents artwork

